Trop J Nat Prod Res, January 2026; 10(1): 6620 – 6630

ISSN 2616-0684 (Print)
ISSN 2616-0692 (Electronic)

Tropical Journal of Natural Product Research

Available online at https://www.tjnpr.org

Original Research Article

Molecular Docking of *Piper betle* L. Compounds against Sortase A and *In Vitro* Evaluation of Antibacterial and Antioxidant Activities

Adit W Santoso[1], Agus Limanto[2]*, Adelina Simamora[2]

[1]*Department of Biology, Faculty of Medicine and Health Sciences, Krida Wacana Christian University, Jakarta, Indonesia*
[2]*Department of Biochemistry, Faculty of Medicine and Health Sciences, Krida Wacana Christian University, Jakarta, Indonesia*

ARTICLE INFO

Article history:
Received 09 October 2025
Revised 11 November 2025
Accepted 07 January 2026
Published online 01 February 2026

ABSTRACT

The rise of antibiotic-resistant *Staphylococcus aureus* necessitates novel antivirulence strategies. Sortase A (SrtA), a key virulence factor, is an attractive target. *Piper betle* L., a medicinal plant with diverse bioactivities, is a potential source of natural SrtA inhibitors. This study aimed to identify such compounds through *in silico* analysis and to evaluate the antioxidant and antibacterial potential of *P. betle* via *in vitro* assays. Nine bioactive compounds were screened using molecular docking, absorption, distribution, metabolism, excretion, and toxicity prediction; and molecular dynamics (MD) simulation (CABS-flex 2.0). Acetyleugenol exhibited the strongest binding to SrtA (S score = -5.98 kcal/mol), favorable drug-likeness, high predicted intestinal absorption, and low blood-brain barrier permeability. MD simulations showed that acetyleugenol stabilized the catalytic residue Cys184 with a root mean square fluctuation = 0.261 Å, comparable with that of the native substrate. Other compounds such as chavicol, showed similar stability, although safrole raised toxicity concerns. *In vitro*, the ethanol extract of *P. betle* showed strong antioxidant activity with IC_{50} values of 6.49 µg/mL (DPPH) and 9.31 µg/mL (ABTS). The extract also demonstrated antibacterial activity against *Streptococcus mutans*, with a minimum inhibitory concentration of 0.31 mg/mL. Studies on the mechanism of the antibacterial effect showed increased DNA and protein leakage in the extracellular fluid, indicating membrane disruption owing to *P. betle* extract. Overall, acetyleugenol is a promising SrtA inhibitor, while *P. betle* extract displays potent antioxidant and antibacterial effects. These findings highlight the therapeutic potential of *P. betle* and its compounds as antimicrobial agents.

Keywords: Acetyleugenol, DNA leakage, *Piper betle*, Protein leakage, *Sortase A*, Molecular docking.

Introduction

Antimicrobial resistance (AMR) occurs when bacteria, fungi, or parasites no longer respond to antimicrobial agents, causing standard treatments to be ineffective and making infections harder to treat. This issue has escalated into a global public health crisis, leading to 1.27 million deaths directly linked to drug-resistant infections and approximately 4.95 million deaths associated with AMR in 2019 alone.[1] The WHO Global Antimicrobial Resistance Surveillance System data reveal trends concerning AMR in Indonesia. For instance, 79% of *Klebsiella pneumoniae* isolates from bloodstream infections were resistant to third-generation cephalosporins, 40% of *Staphylococcus aureus* strains were methicillin-resistant (MRSA), and 51% of *Acinetobacter species* displayed carbapenem resistance.[2] *Staphylococcus aureus* is a significant human pathogen responsible for various infections, ranging from minor skin conditions to life-threatening illnesses such as pneumonia and sepsis.[3] MRSA emergence highlights the urgent need for innovative therapies that bypass traditional resistance pathways. Targeting virulence factors, such as Sortase A (SrtA), an enzyme critical for bacterial adhesion and colonization, offers a promising strategy for reducing the selective pressure that drives resistance.[4, 5] Sortase A (SrtA) is a membrane-bound cysteine transpeptidase that anchors virulence-associated surface proteins to the bacterial cell wall by cleaving the LPXTG sorting motif in precursor proteins.[5] Its catalytic activity relies on three conserved residues, namely, His120, Cys184, and Arg197, with Cys184 being essential. Modifications to Cys184 eliminate enzymatic function, confirming its role as a cysteine protease.[5, 6] SrtA forms a thioester intermediate during catalysis, which is resolved by the pentaglycine cross-bridge in the peptidoglycan layer, leading to a stable amide linkage that permanently attaches the protein; this process is vital for tissue colonization and biofilm development.[6] In addition to systemic pathogens such as *S. aureus*, oral pathogens such as *Streptococcus mutans* pose significant health challenges. *S. mutans* is a key contributor to dental caries, as it is capable of forming biofilms and producing acid that demineralizes tooth enamel.[7] Beyond its role in oral disease, *S. mutans* has been associated with extraoral infections, including infective endocarditis and atherosclerosis, owing to its ability to enter the bloodstream during dental procedures.[8] The persistence and pathogenicity of *S. mutans* are closely linked to its capacity for biofilm formation and resistance to environmental stress, including oxidative damage.[9] Given the rising concern over biofilm-related infections, there is a growing interest in natural compounds that can disrupt bacterial membranes, inhibit virulence mechanisms, and provide antioxidant protection. Natural products continue to be valuable sources of novel antimicrobial agents because of their structural diversity and bioactive potential. *Piper betle L.* (green betel leaf), commonly used in traditional medicine throughout Southeast Asia, including Indonesia, contains bioactive compounds such as eugenol and chavicol, which exhibit antimicrobial, anti-inflammatory, and antioxidant properties.[10]

*Corresponding author. Email: agus.limanto@ukrida.ac.id
Tel: +62-817-6777781

Citation: Santoso WA, Limanto A, Simamora A. Molecular Docking of *Piper betle* L. Compounds Against Sortase A and *In Vitro* Evaluation of Antibacterial and Antioxidant Activities. Trop J Nat Prod Res. 2025; 10(1): 6620 – 6630 https://doi.org/10.26538/tjnpr/v10i1.27

Official Journal of Natural Product Research Group, Faculty of Pharmacy, University of Benin, Benin City, Nigeria

This study explores the inhibitory potential of bioactive compounds from *Piper betle L.* against SrtA in *S. aureus* using molecular docking analysis and absorption, distribution, metabolism, excretion, and toxicity (ADMET) prediction models. By focusing on virulence rather than bacterial viability, this approach may provide new therapeutic strategies to combat AMR. In addition, the antioxidant and antibacterial activities of *Piper betle* ethanol extract were assessed *in vitro*, including its efficacy against *S. mutans* and its possible membrane-disruptive mechanism of action. These findings may provide insight into the therapeutic potential of *Piper betle* as a natural source of multifunctional agents to address bacterial virulence and oxidative stress.

Materials and Methods

Chemicals and bacterial materials

2,2-diphenyl-1-picryl-hydrazyl (DPPH) and 2,2'-azino-bis(3-ethylbenzothiazoline-6-sulfonic acid) (ABTS)**,** $K_2S_2O_8$ were purchased from Sigma-Aldrich (St. Louis, USA). *Streptococcus mutans* ATCC 14721 was obtained from the Laboratory of Microbiology, Krida Wacana Christian University, Indonesia.

Methods

Docking studies

Identification of bioactive compounds in Piper betle L.

Bioactive compounds from *Piper betle L.* leaves were identified through specialized phytochemical databases, including the Taiwan Traditional Chinese Medicine Database (http://tcm.cmu.edu.tw/), IJAHdb (http://ijah.apps.cs.ipb.ac.id), and HERBALdb (http://herbaldb.farmasi.ui.ac.id/).[11, 12] The canonical Simplified Molecular Input Line Entry System (SMILES) notations of each compound were validated against the PubChem database to ensure structural accuracy. Ligands were initially drawn in a two-dimensional (2D) format using MarvinSketch and subsequently converted into energy-minimized three-dimensional (3D) structures using Open Babel (v.2.4.1).

Protein preparation and molecular docking

The 3D crystal structure of SrtA from *Staphylococcus aureus* was retrieved from the Protein Data Bank (PDB ID: 1T2W and 1T2P). Protein preparation was performed using MOE 2022.02, involving the removal of crystallographic water molecules and irrelevant heteroatoms, the assignment of protonation states using Protonate3D at pH 7.4, and energy minimization using the AMBER10:EHT force field.[13] The active site was defined based on the co-crystallized LPXTG peptide in the 1T2W structure, specifically targeting the conserved catalytic residues His120, Cys184, and Arg197.

Prepared ligands were imported into the MOE, and the energy was minimized and docked into the defined active site using the Dock module. The Triangle Matcher algorithm was used for placement, with London dG as the initial scoring function and Induced Fit as the refinement protocol. Final binding affinities were estimated using the GBVI/WSA dG scoring function.[13] The LPXTG peptide served as a positive control for comparative analysis.

Post-Docking analysis

Top-ranked docking poses were analyzed using MOE's interaction analysis tools to assess the hydrogen bonding, hydrophobic interactions, and involvement of catalytic residues. Compounds exhibiting high binding affinity and favorable interaction profiles relative to the LPXTG peptide were selected for further evaluation.

ADMET and drug-likeness prediction

The drug-likeness and pharmacokinetic profiles of the selected bioactive compounds from *Piper betle* L. were systematically evaluated using a combination of computational tools. Initially, the canonical SMILES of each compound was retrieved from the PubChem database and submitted to the SwissADME web server (http://www.swissadme.ch/) to assess compliance with Lipinski's Rule of Five, which considers molecular weight, lipophilicity (log*P*), hydrogen bond donors and acceptors, and molar refractivity as indicators of oral bioavailability potential.[12]

Subsequently, detailed ADMET predictions were conducted using the pkCSM platform (http://biosig.unimelb.edu.au/pkcsm/), which utilizes graph-based signatures to estimate pharmacokinetic and toxicity properties.[13] Absorption parameters included human intestinal absorption (HIA), Caco-2 permeability, and P-glycoprotein (P-gp) substrate and inhibitor status to infer oral bioavailability and potential efflux liability. Distribution characteristics were evaluated through predictions of blood-brain barrier (BBB) permeability and the volume of distribution at steady state (VDss). Metabolic interactions were assessed by predicting inhibitory effects on the major cytochrome P450 isoforms: CYP1A2, CYP2C19, CYP2C9, CYP2D6, and CYP3A4. Excretion potential was determined via total clearance (CLtot), whereas toxicity was predicted based on AMES mutagenicity and hepatotoxicity.[13]

Molecular dynamics (MD) simulation

MD simulations were employed to assess the structural stability and flexibility of the SrtA ligand complexes under dynamic conditions. The simulations were conducted using the CABS-flex 2.0 web server (http://biocomp.chem.uw.edu.pl/CABSflex2), a coarse-grained modeling platform designed to simulate protein backbone fluctuations.[14]

The top three ligand-bound complexes—acetyleugenol, methyleugenol, and chavibetol—were selected based on their docking scores and key interactions with residues in the SrtA active site. Each complex was submitted in PDB format, with ligand coordinates integrated into the protein structure file.

CABS-flex simulations were performed using the default parameters, which included 50 simulation cycles and a simulation temperature of 1.4 (dimensionless units). Global distance restraints were automatically applied to maintain the overall protein fold while allowing local conformational flexibility. The output consisted of multiple conformational models representing thermodynamically feasible structures of the protein–ligand complex.

Post-simulation analysis involved calculating root mean square fluctuation (RMSF) values for each residue, facilitating a comparative evaluation between the unbound (apo) and ligand-bound SrtA forms. The flexibility of the catalytic triad residues (His120, Cys184, and Arg197) and ligand-contact residues such as Val168 and Ile199, which are critical for enzymatic function and inhibitor binding. Structural deviations and conformational shifts were visualized using PyMOL and UCSF Chimera, to assess binding-induced stabilization and interaction persistence throughout the simulation.

In vitro analysis of P. betle extract

Extract preparation

Leaves of *P. betle* were obtained from the local market in Jakarta, Indonesia (coordinates: -6.175946662482058, 106.78365707878369) in October 2025. The leaves were identified by Prof Kris H. Timotius of Krida Wacana Christian University. A voucher specimen was deposited in the research laboratory at Krida Wacana Christian University (a voucher number KWSC 0063). After thoroughly cleaning the leaves, they were dried using a food dehydrator at 40 °C for several days. The dried leaves (20 g) were macerated using 96% ethanol in a 1:10 ratio for 72 h. The filtrate was obtained by filtering through a filter paper, after which the solvent was evaporated using a Buchi R II rotary evaporator (Buchi Labortechnik, Switzerland). The dried extract obtained was 3.02 g (yield 15.10%), and was stored at 4 °C before use.

Antibacterial activity assays

Determination of bacterial inhibition zone

Antibacterial effect of the ethanol extract of *P. betle* leaves was assayed by an agar well diffusion method on *Streptococcus mutans* ATCC 14721 based on a previously reported method.[14] The bacterial inoculum (0.5 McFarland turbidity standard, 100 µL) was spread evenly into an agar plate, thereafter, followed by the addition of molten Muller-Hinton agar (OXOID CM0337). Subsequently, a 5-mm well was made on the plate and suspended with the ethanol solution of *P. betle* extract (20 µL). Plates were incubated at 37 ℃ for 24 h. Ethanol was used as the negative control.

ISSN 2616-0684 (Print)
ISSN 2616-0692 (Electronic)

Determination of minimum inhibitory concentration (MIC)
Antibacterial activity of the ethanol extract of *P. betle* leaves was further tested by analyzing the MIC against *S mutans*. A broth dilution method was applied using a 96-U-bottom plate.[14] A 100 µL of extract solution prepared in ethanol was pipetted into the first column of the well. To all other wells, 50 µL of Muller-Hinton broth was added. Inoculum of the maximum 24 h old was adjusted to 0.5 McFarland turbidity standard using a BioSan Den-1B. Bacterial suspension was prepared by adding the inoculum to a 1:20 water: Tween 80 solution. Into each well was pipetted 10 µL of the bacterial suspension. Serial dilution of the extract solution was then performed by taking 50 µL of the extract solution which was serially diluted in a descending concentration to obtain different concentration points. The reaction mixture was incubated for 24 h at 37 °C. The negative control was prepared using the same reaction mixture, but without the extract. The solvent toxicity was tested using ethanol instead of the extract. The MIC was determined as the lowest concentration of *P. betle* extract in which no obvious turbidity was observed.

Evaluation of DNA leakage
DNA leakage was analyzed using a previously reported method.[15] *S. mutans* cells were treated with 0, 25, 50, and 100 µL of *P. betle* ethanol extract of 1.25 mg/mL, diluted into 10 mL solution with Muller-Hinton broth. The mixture was incubated for 12 h. After incubation, the tubes were centrifuged at 10000 rpm for 15 min. The supernatant was collected and analyzed at 260 nm using a spectrophotometer. An OD of 1 refers to the leakage of 50 µg/mL of DNA.[15] Blank solutions were prepared using *P. betle* ethanol extract of each dilution without the addition of *S. mutans* cells.

Evaluation of protein leakage
Protein leakage was analyzed using a Bradford assay based on a previously reported method.[16] *S. mutants* cells were treated with 0, 25, 50, and 100 µL of *P. betle* extract (1.25 mg/mL), and diluted into a 10 mL solution with Muller-Hinton broth. The mixture was incubated for 12 h. After incubation, the tubes were centrifuged at 10000 rpm. The supernatant of each concentration point (50 µL) was mixed with the Bradford reagent (150 µL), and then incubated in the dark for 10 min. The absorbance was measured at 595 nm. Bovine serum albumin was used to generate a standard curve for the determination of protein content.

Antioxidant activity assays
Determination of 1,1-diphenyl-2-picryl-hydrazyl (DPPH) radical scavenging activity
The scavenging activity of the plant extract on DPPH radicals was determined based on the reported method.[17] Typically, in a flat bottom 96-well, plant extract of different concentrations (50 µL) were added into the wells. DPPH solution in ethanol (0.6 mM, 80 µL) was added to each well. The reaction mixture was mixed and incubated at 27 °C for 30 min at 250 RPM in a shaking incubator (Thermostar BMG Labtech). The absorbance was measured at 520 nm using a BioRad iMark plate reader (Hercules, CA, USA). The percentage of inhibition was calculated as follows: inhibition (%) = $((A_{control} - A_{sample})/ A_{control}) \times 100$, where $A_{control}$ was the absorbance of DPPH solution without sample and A_{sample} was the absorbance of DPPH solution with the samples. Activity was presented as an IC50 value, calculated by the linear regression equation from the plot of inhibition percentage against plant extract concentration. The experiment was conducted in triplicates. Result was compared with positive control ascorbic acid.

Determination of 2,2'-azino-bis(3-ethylbenzothiazoline-6-sulfonic acid) (ABTS) radical scavenging activity
The scavenging activity of the plant extract on $ABTS^{\bullet+}$ was determined using previous method with slight modifications.[18] The $ABTS^{\bullet+}$ radicals were generated by mixing ABTS solution (7 mM) and potassium persulphate (2.45 mM), thereafter was incubated for 12-16 h in the dark at ambient temperature. Before the reaction, the absorbance of the $ABTS^{\bullet+}$ solution was adjusted to around 0.700 ± 0.002 by diluting the solution with phosphate buffered saline (10 mM, pH 7.4). For the assay, the $ABTS^{\bullet+}$ solution (180 µL) was reacted with the plant extract solution of different concentrations (20 µL) in a flat bottomed 96-well. The mixture was incubated at 27 °C for 5 min at 250 RPM in a shaking incubator (Thermostar BMG Labtech). The absorbance was measured at 750 nm using a BioRad iMark plate reader (Hercules, CA, USA). The percentage of radical scavenging activity was calculated as follows: inhibition (%) = $((A_{control} - A_{sample})/ A_{control}) \times 100$, where $A_{control}$ was the absorbance of $ABTS^{\bullet+}$ solution without the sample and A_{sample} was the absorbance of $ABTS^{\bullet+}$ solution with the samples. The IC_{50} value (µg/mL) of the sample was calculated using the linear regression equation obtained by plotting the inhibition percentage with the sample concentration. The experiment was conducted in triplicate.

Results and Discussion

Molecular docking analysis
Identification of bioactive compounds in P. betle L.
Nine bioactive compounds were identified from *Piper betle* L. leaves through comprehensive screening of phytochemical databases, including the Taiwan Traditional Chinese Medicine Database, IJAHdb, and HERBALdb.[11, 12] Structural verification and standardization were performed using the PubChem database. The selected compounds predominantly belong to the phenylpropanoid and methoxyphenol classes, with one representative sesquiterpene, highlighting the chemical diversity of *P. betle*.
Several compounds, such as eugenol, chavicol, and estragole, are well-documented for their broad-spectrum antibacterial activity.[19] Hydroxychavicol, a key constituent of *P. betle* extracts, possesses antibacterial activity.[20] Methyleugenol, acetyleugenol, and chavibetol are structural analogs of eugenol, featuring modifications that may influence their binding affinity and specificity toward microbial targets. The inclusion of β-caryophyllene, a bicyclic sesquiterpene with a hydrocarbon scaffold distinct from phenolic derivatives, contributes to the structural diversity and offers an alternative pharmacophore for potential interaction with the SrtA binding pocket.
This curated library was used as the ligand dataset for subsequent virtual screening against SrtA through molecular docking, ADMET prediction, and MD simulation. Table 1 summarizes the compound names, SMILES notations, and PubChem CIDs.

Table 1: Curated bioactive compounds from *P. betle L.*

No.	Compound Name	SMILES	PubChem CID
1	Hydroxychavicol	C=CCC1=CC(=C(C=C1)O)O	70775
2	Chavicol	C=CCC1=CC=C(C=C1)O	68148
3	Chavibetol	COC1=C(C=C(C=C1)CC=C)O	596375
4	Eugenol	COC1=C(C=CC(=C1)CC=C)O	3314
5	Methyleugenol	COC1=C(C=C(C=C1)CC=C)OC	7125
6	Acetyleugenol	CC(=O)OC1=C(C=C(C=C1)CC=C)OC	596380
7	Estragole	COC1=CC=C(C=C1)CC=C	8815
8	β-Caryophyllene	C/C/1=C\CCC(=C)[C@H]2CC([C@@H]2CC1)(C)C	5281515
9	Safrole	C=CCC1=CC2=C(C=C1)OCO2	5144

Molecular docking results
The binding affinity of *P. betle* L. bioactive compounds toward SrtA was evaluated using molecular docking, with the LPXTG peptide as a positive control to confirm correct pocket recognition. Lower (more negative) S scores indicate stronger predicted binding, and poses with RMSD_refine ≤ 2.0 Å were considered reliable.
The LPXTG peptide showed the strongest binding affinity, with docking scores ranging from -7.60 to -7.63 kcal/mol and RMSD values between 1.52 and 2.22 Å, forming multiple hydrogen bonds to Glu105, Asp112, Ser116, and Thr180, and ionic interactions with Glu105,

ISSN 2616-0684 (Print)
ISSN 2616-0692 (Electronic)

Glu108, and Arg197, consistent with specific recognition within the SrtA active site.

Among the *P. betle* compounds, acetyleugenol exhibited the best ligand performance (S = –5.98 kcal/mol; RMSD = 0.88 Å), with π–H interactions to Val168 and Ile199. Methyleugenol followed with a docking score of –5.39 kcal/mol and interactions involving Val168 and Ile199.

Estragole, eugenol, and chavibetol demonstrated moderate binding scores (S ≈ -5.28 to -5.15 kcal/mol), dominated by hydrophobic contacts with Val168 and Ile199. Hydroxychavicol scored slightly lower (S = -4.89 kcal/mol), forming one hydrogen bond to Leu169, suggesting possible steric hindrance in the hydrophobic pocket. The sesquiterpene β-caryophyllene gave S = -5.37 to -5.10 kcal/mol with acceptable RMSD values, consistent with hydrophobic accommodation without polar contacts. Chavicol and safrole exhibited the weakest binding profiles (S = -5.18 to -4.60 kcal/mol) with limited interaction with the catalytic residues. Table 2 summarizes the detailed results, including the best docking score, RMSD_refine, and interaction residues for each compound.

Table 2: Docking results of bioactive compounds in *Piper betle* L. with SrtA.

No	Compound	S Score (kcal/mol)	RMSD (Å)
1	LPXTG	-7.6327	2.2189
2	Acetyleugenol	-5.9821	0.8818
3	Methyleugenol	-5.3857	1.3882
4	Chavibetol	-5.2069	0.8224
5	Safrole	-5.1521	0.6793
6	Eugenol	-5.1475	2.8892
7	Estragole	-5.1156	1.4538
8	*β*-Caryophyllene	-5.1022	1.5888
9	Hydroxychavicol	-4.84354	1.4659
10	Chavicol	-4.6639	1.4845

ADMET and drug-likeness prediction

The pharmacokinetic and toxicity profiles of nine bioactive compounds from *P. betle* L. were assessed using the SwissADME and pkCSM platforms. The evaluation encompassed key parameters related to ADMET and drug-likeness using Lipinski's Rule of Five.

All compounds met Lipinski's Rule criteria, except β-caryophyllene, which violated the lipophilicity parameter (logP > 5). This indicates good oral bioavailability potential for most compounds, supporting their viability as drug candidates.

HIA was high across all compounds, with values exceeding 91%, indicating favorable oral absorption. Caco-2 permeability values (log Papp) ranged from 1.41 to 1.78, suggesting moderate-to-high intestinal epithelial permeability. None of the compounds were predicted to be substrates or inhibitors of P-glycoprotein (P-gp), thereby reducing the risk of efflux-mediated bioavailability reduction.

All compounds demonstrated moderate BBB permeability, with β-caryophyllene showing the highest value (log BB = 0.733), indicating potential central nervous system (CNS) penetration. VDss was variable, with *β*-caryophyllene and hydroxychavicol showing higher tissue distribution (log VDss > 0.4), whereas acetyleugenol had the lowest (-0.007), suggesting limited tissue dispersion.

Most compounds were not predicted to inhibit major cytochrome P450 enzymes. However, chavicol, chavibetol, eugenol, methyleugenol, estragole, and safrole were predicted to inhibit CYP1A2, indicating potential metabolic interaction risks. None of the compounds were CYP2C19, CYP2C9, CYP2D6, or CYP3A4 inhibitors, minimizing the likelihood of broader drug–drug interactions.

Total clearance rates varied, with β-caryophyllene showing the highest predicted clearance (log CL = 1.088 mL/min/kg) and safrole the lowest (log CL = 0.116 mL/min/kg). These differences may influence the plasma half-life and dosing frequency in vivo.

Toxicological predictions revealed that most compounds were non-mutagenic in the AMES test and exhibited no hepatotoxicity. Exceptions included chavibetol, eugenol, methyleugenol, estragole, and safrole, all of which were flagged as potential AMES mutagens. Additionally, safrole was predicted to exhibit hepatotoxicity, warranting caution in its further development.

MD simulation

MD simulations were performed using the CABS-flex 2.0. As a coarse-grained, backbone-level approach, CABS-flex reports per residue. RMSF as an indicator of local flexibility; it does not provide binding thermodynamics, therefore RMSF trends are interpreted as modeled flexibility changes and should be confirmed by all-atom MD where needed. Analyses focused on the catalytic triad (His120, Cys184, and Arg197) which are essential for enzymatic activity (Figure 2).

The LPXTG control peptide showed low RMSF at the catalytic residues (His120 = 0.447 Å, Cys184 = 0.231 Å, and Arg197 = 0.395 Å), consistent with a constrained active-site backbone. Among the tested compounds, acetyleugenol demonstrated the closest match to the control, lowering backbone motion at Cys184 (0.261 Å) and showing moderate Arg197 (0.498 Å), whereas His120 remained more mobile (0.788 Å). Methyleugenol showed lower fluctuations at His120 (0.484 Å) and Arg197 (0.376 Å), with a modestly higher Cys184 (0.675 Å), indicating a residue-specific flexibility pattern rather than uniform stabilization. Chavibetol, eugenol, and caryophyllene also displayed moderate RMSF values (generally < 0.55 Å at key positions), whereas hydroxychavicol and estragole showed higher RMSF values at Cys184 and Arg197, suggesting less constrained backbones in the catalytic region within this model. Safrole exhibited a low RMSF at Cys184 (0.146 Å) and higher RMSF at Arg197 (0.430 Å) but is deprioritized owing to the predicted safety liabilities from the ADMET screening.

Overall, the RMSF patterns are consistent with the docking-derived poses that engage the catalytic region, nominating acetyleugenol and methyleugenol as the most compelling candidates from a flexibility-based perspective. A summary of the MD results is presented in Table 4.

Antibacterial activity of P. betle extract

Antibacterial activity of *P. betle* leaf extract was tested against *S. mutans* by measuring the inhibition zone diameter. As shown in Figure 3, *S. mutans* was sensitive against *P. betle* extract with an inhibition diameter zone of 1.34 ± 0.11 cm.

The MIC and MBC assays were included in this study to determine the lowest concentration of *P. betle* extract that inhibited and killed the bacterium, respectively. The results are presented in Table 5.

A DNA leakage assay was conducted to further evaluate the mechanism of the observed antibacterial activity against *S. mutants*. The graphs in Figure 4 represent the amount of DNA (A) and protein (B) identified in the supernatant of *S. mutans* following treatment with different concentrations of *P. betle* extract. The OD reading at 260 nm demonstrated the presence of DNA in the supernatant of *S. mutans* following treatment with *P. betle* extract (Figure 4A). At each concentration (0.05, 0.1, and 0.2 mg/mL), significant differences in DNA leakage were observed between the negative control (only ethanol) ($p < 0.05$) and the tested concentrations ($p < 0.05$). Notably, the DNA leakage was found to be concentration dependent, with a

ISSN 2616-0684 (Print)
ISSN 2616-0692 (Electronic)

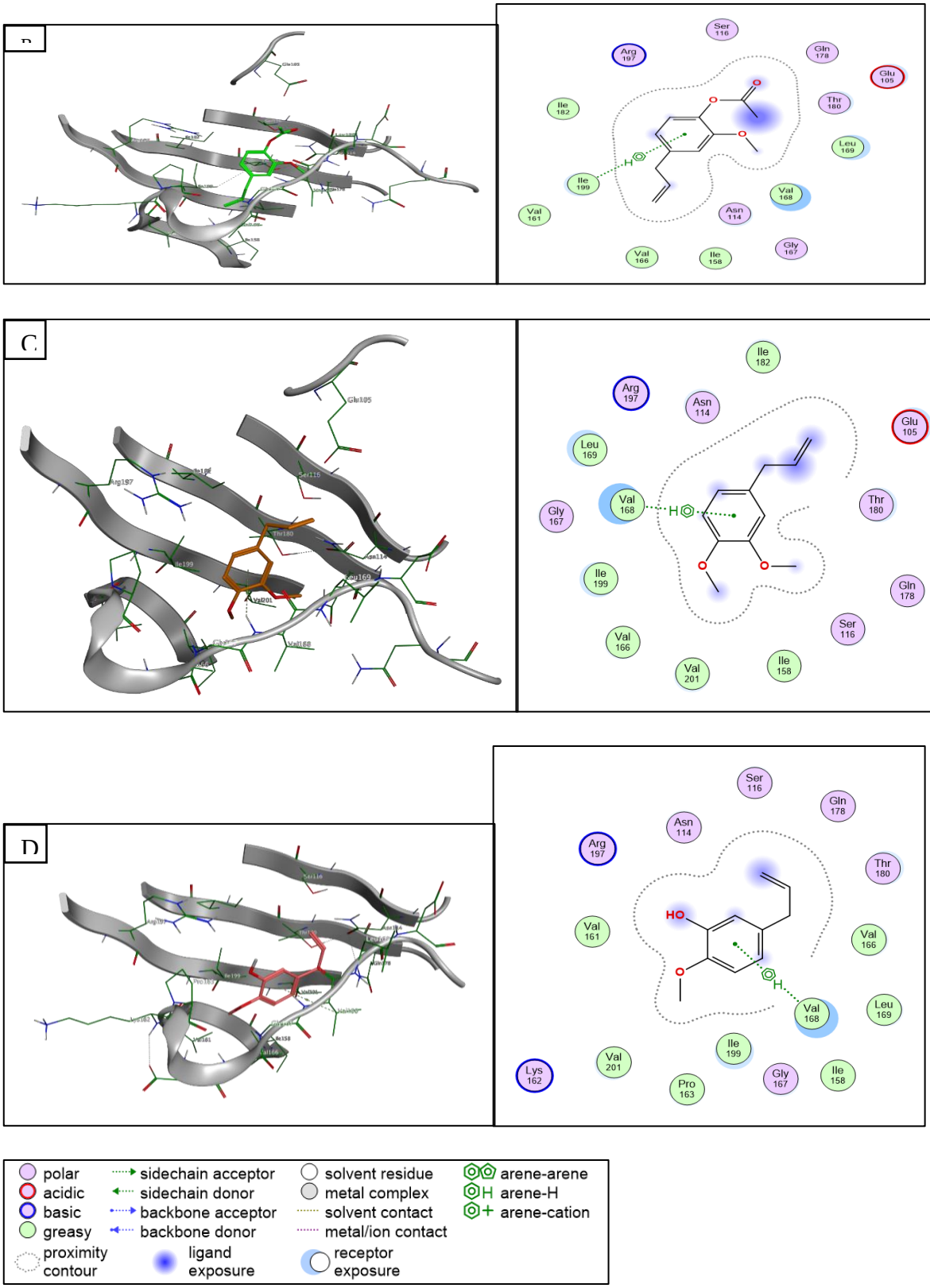

Figure 1: Docking Interaction of SrtA with LPXTG and Top *Piper betle* L compounds. 3D and 2D interactions diagrams of Srt A with LPXTG (A), Acetyleugenol (B), Methyleugenol (C), and Chavibetol (D), showing key binding residues and interaction types. Interaction types are illustrated to the accompanying legend.

ISSN 2616-0684 (Print)
ISSN 2616-0692 (Electronic)

Table 3: ADMET screening of potential SrtA inhibitors from *P. betle* L

Compound	Lipinski's Rule Compliance	Absorption	Distribution	Metabolism	Excretion	Toxicity
		HIA (%); Caco-2 permeability (log Papp); P-gp-substrate; P-gp inhibitor	BBB permeability (log BB); VDss (log L/kg)	CYP3A4 substrate; CYP3A4 inhibitor; CYP2D6 substrate; CYP2D6 inhibitor	Total Clearance (log mL/min/kg)	AMES Toxicity; Hepatotoxicity
Hydroxychavicol	0	92.09; 1.676; No; No	0.361; 0.477	No; No; No; No	0.206	No; No
Chavicol	0	93.41; 1.607; No; No	0.476; 0.465	No; No; No; No	0.257	No; No
Chavibetol	0	91.83; 1.497; No; No	0.389; 0.203	No; No; No; No	0.28	Yes; No
Eugenol	0	92.04; 1.559; No; No	0.374; 0.240	No; No; No; No	0.282	Yes; No
Methyleugenol	0	94.53; 1.528; No; No	0.422; 0.264	No; No; No; No	0.338	Yes; No
Acetyleugenol	0	94.75; 1.659; No; No	0.401; -0.007	No; No; No; No	0.468	No; No
Estragole	0	94.53; 1.410; No; No	0.601; 0.401	No; No; No; No	0.332	Yes; No
β-Caryophyllene	1 (logP >5)	94.84; 1.423; No; No	0.733; 0.652	No; No; No; No	1.088	No; No
Safrole	0	96.31; 1.784; No; No	0.300; 0.283	No; No; No; No	0.116	Yes; Yes

Table 4: Molecular dynamics results of bioactive compounds in *P. betle* L. with SrtA

No	Compound	RMSF_120	RMSF_184	RMSF_197
1	LPXTG	0.447	0.231	0.395
2	Acetyleugenol	0.788	0.261	0.498
3	Methyleugenol	0.484	0.675	0.376
4	Chavibetol	0.569	0.377	0.520
5	Safrole	0.323	0.146	0.43
6	Eugenol	0.392	0.384	0.514
7	Estragole	0.674	0.456	0.306
8	*β*-Caryophyllene	0.419	0.421	0.338
9	Hydroxychavicol	0.638	0.474	0.538
10	Chavicol	0.208	0.289	0.402

higher extract concentration giving rise to a higher amount of DNA, indicating more pronounced leakage from *S. mutans* cells.
Similarly, the supernatant of *S. mutans* showed positive results when tested with the Bradford reagent. As in the DNA test, the protein amount analyzed was in accordance with the concentration of *P. betle* extract. These results indicate that cell membrane damage caused intracellular protein leakage into the extracellular environment.

Antioxidant activity of P. betle leaf extract
Radical scavenging activity of *P. betle* extract was determined using DPPH and ABTS assays. Both assays were frequently used to evaluate the antioxidant properties of plant extracts, which may contain hydrophilic, lipophilic, and pigmented antioxidant compounds. Table 5 summarizes the results. In the DPPH assay, the *P. betle* ethanol extract exhibited an IC_{50} value of 6.49 ± 0.01 µg/mL, which was significantly lower than that of Trolox (7.55 ± 0.08 µg/mL; $p < 0.05$), indicating a stronger free-radical scavenging capacity. Similar observation was reported by other researchers obtaining strong DPPH scavenging activity for the ethanol extract of *P. betle* (3.48 µg/mL).[21] Similarly, in the ABTS assay, strong scavenging activity (9.31 ± 0.34 µg/mL) was observed for *P. betle* extract as compared with Trolox (3.29 ± 0.03 µg/mL).

Molecular docking analysis
To effectively inhibit the SrtA enzyme, bioactive compounds from *P. betle* L. should exhibit favorable interactions within the catalytic region relative to reference ligands, the LPXTG peptide, acknowledging the comparative limitations of the docking scores. Computational docking analysis identified several promising inhibitors with low RMSD values, indicating consistent and convergent binding poses within the SrtA

ISSN 2616-0684 (Print)
ISSN 2616-0692 (Electronic)

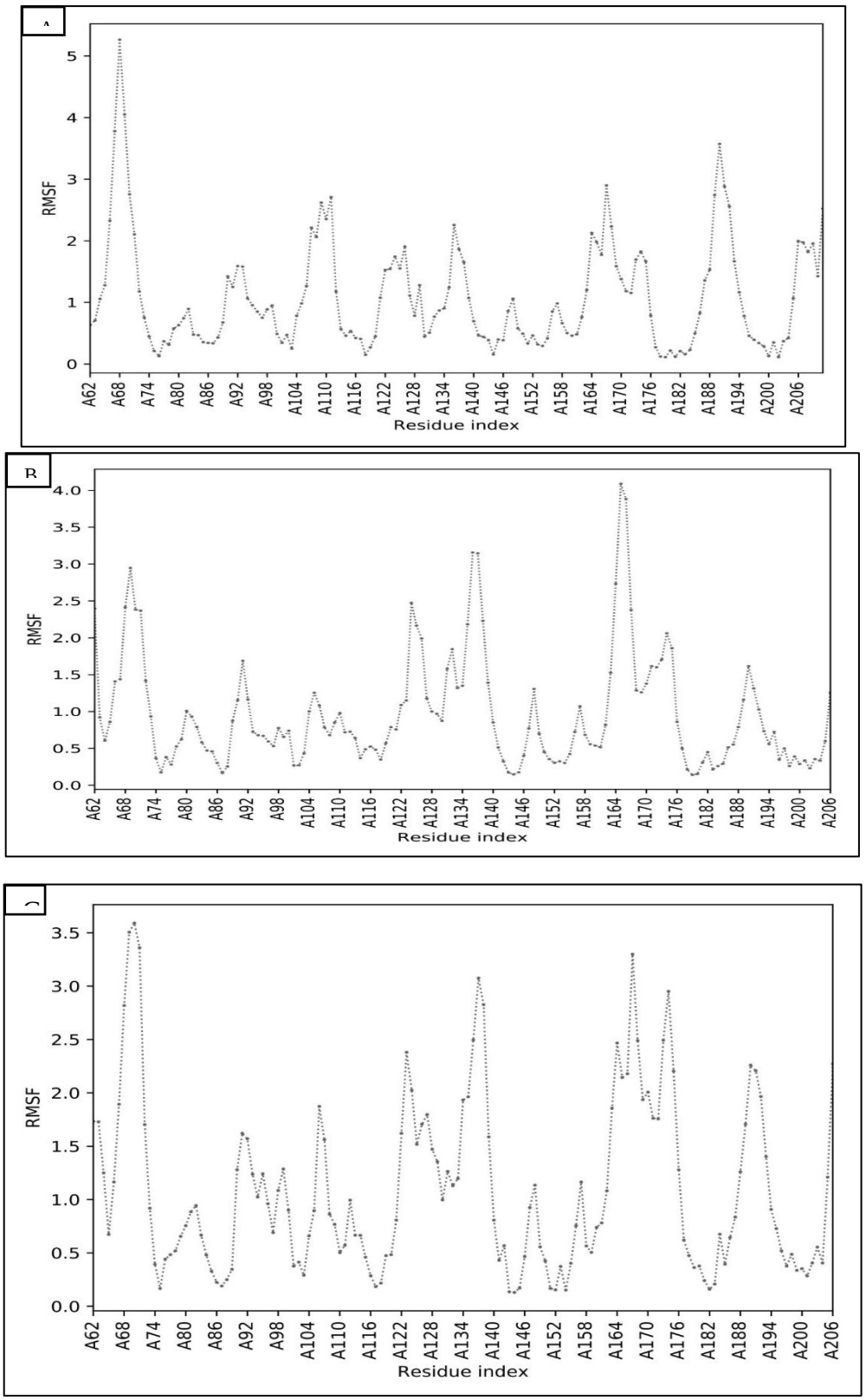

ISSN 2616-0684 (Print)
ISSN 2616-0692 (Electronic)

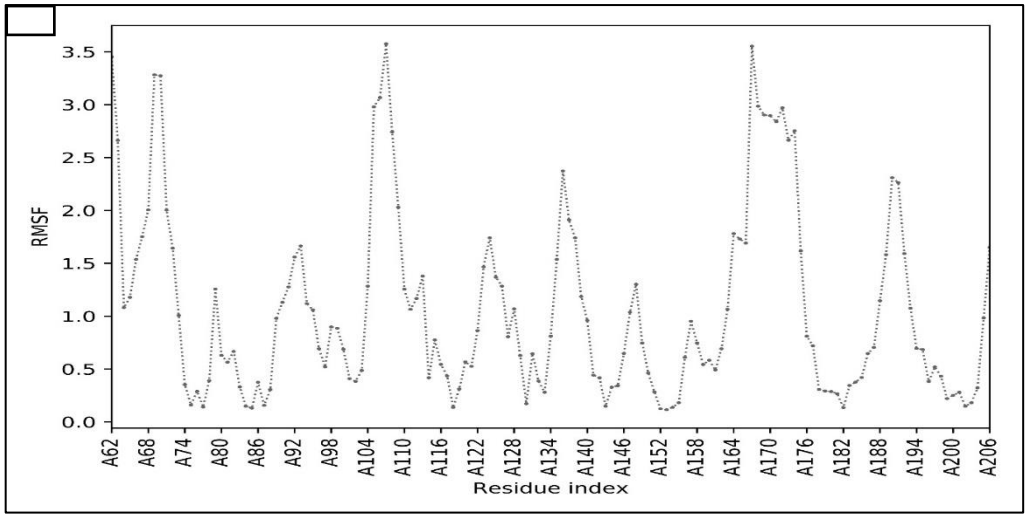

Figure 2: Root Mean Square Fluctuation (RMSF) profiles of Sortase A (SrtA) backbone residues during molecular dynamics simulations using CABS-flex. (A) SrtA bound to LPXTG motif; (B) SrtA bound to acetyleugenol; (C) SrtA bound to methyleugenol; (D) SrtA bound to chavibetol. The plots represent residue-wise backbone flexibility, where higher RMSF values indicate greater structural fluctuations. Binding of *Piper betle* derivatives results in different dynamic behaviors compared to the control.

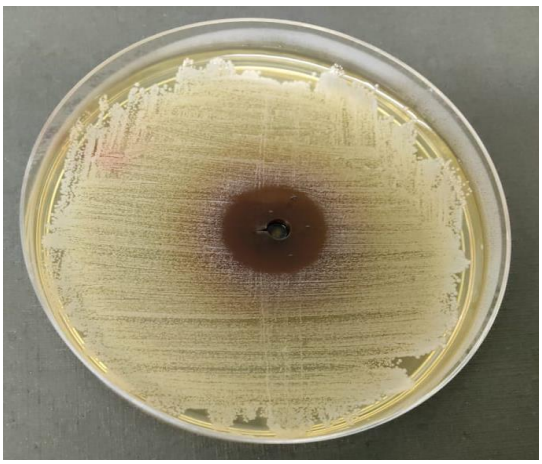

Figure 3: Inhibition zone of *P. betle* ethanol extract against *S. mutans*.‡
‡Zone diameter was determined by the agar disc diffusion method at 0.5 McFarland turbidity standard after 24 h incubation time at 37 °C. A cork borer set No. 2 was used for the well.

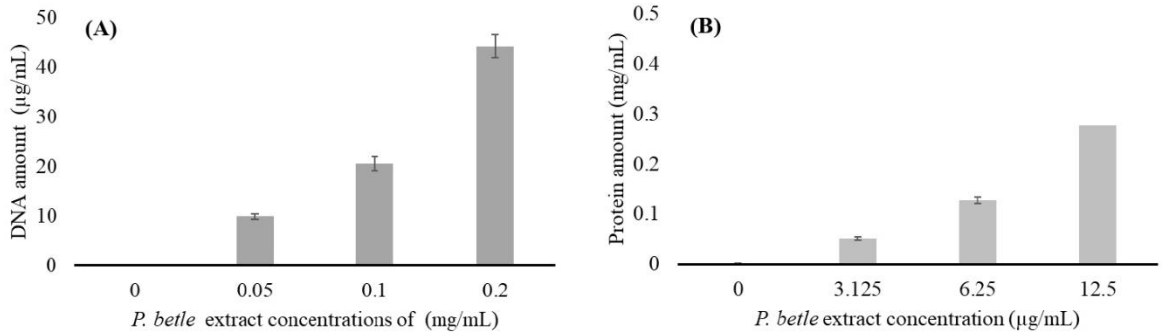

Figure 4: The DNA (A) and protein leakage from *S. mutans* in the presence of *P. betle* extract. DNA amount was measured based on OD at 260 nm (OD = 1 equivalent to 50 µg/mL of DNA).

active site. The best-docking molecules share a common allylbenzene scaffold with an aromatic ring and polar functional groups that facilitate an optimal interaction with SrtA.

Eugenol (allyl-2-methoxyphenol) has an aromatic ring, an allyl tail, a free phenolic hydroxyl group (–OH), and a methoxy group (–OCH_3). Docking simulations showed that the benzene rings fit into a hydrophobic pocket in SrtA, forming π-stacking interactions with aromatic amino acids. Meanwhile, the phenolic -OH is positioned to form a hydrogen bond with an active-site residue, mimicking the interactions observed with natural peptide substrate of the enzyme.

Methyleugenol, which is structurally similar to eugenol but with a methoxy group replacing the hydroxyl group, is also predicted to bind favorably to SrtA. Although the methoxy group is a weaker hydrogen bond acceptor, it can still contribute to polar contacts, whereas the rest of the scaffold engages in van der Waals interactions within the SrtA binding cleft. Acetyleugenol, an acetylated derivative of eugenol, is predicted to form additional favorable contacts with SrtA. The ester carbonyl group act as a hydrogen bond acceptor, while the aromatic and alkene moieties preserve the hydrophobic interactions.

Eugenol, methyleugenol, and acetyleugenol exhibited strong binding to the SrtA enzyme, demonstrating that an aromatic ring with an allyl side chain for hydrophobic anchoring, combined with at least one polar substituent capable of hydrogen bonding, constitutes an effective pharmacophore for SrtA engagement. Their significantly more negative docking scores relative to less functionalized analogs highlight the critical role of these functional groups in enhancing binding affinity.

Phenylpropanoids from *P. betle* L. bearing aromatic hydroxyl substituents exhibited favorable predicted affinities, albeit slightly lower than those of the eugenol derivatives. Hydroxychavicol and chavibetol, which possess free phenolic –OH groups, could establish hydrogen bonds within the catalytic pocket in a manner comparable with that of eugenol. Although hydroxychavicol contains two hydroxyl groups, its less favorable docking score suggests suboptimal orientation or spatial positioning of these polar interactions relative to key residues. Nevertheless, its performance surpassed that of the fully hydrophobic analogs, underscoring the critical contribution of phenolic functionality to SrtA recognition and binding stability.

Phenylpropanoids from *P. betle* L. containing aromatic hydroxyl groups also showed favorable docking affinities, although slightly lower than eugenol derivatives. Compounds such as hydroxychavicol and chavibetol, each possessing free phenolic –OH groups, form hydrogen bonds with the enzyme similarly to eugenol. Hydroxychavicol, which has two –OH groups, has a lower docking score, suggesting that the spatial orientation of these groups within the binding site may be suboptimal. Nevertheless, it outperforms fully hydrophobic analogs, underscoring the importance of phenolic hydroxyl functionalities in SrtA binding. Chavibetol, with one –OH and one –OCH_3 group, has a docking score comparable with eugenol, indicating good accommodation of these substituents by the binding pocket. Chavicol, the simplest phenolic with a single hydroxyl group, demonstrates moderate binding affinity owing to aromatic interactions but lacks additional polar substituents to further enhance binding.

Overall, phenolic compounds with at least one free hydroxyl group on the benzene ring tended to improve SrtA binding, and additional small polar substituents may further enhance affinity. In contrast, more hydrophobic molecules or those with single, less interactive substituents show weak binding to SrtA. For instance, estragole lacks a phenolic –OH group and relies predominantly on van der Waals forces, resulting in lower docking scores than eugenol. Safrole also demonstrates weak binding attributed to the inability of its methylenedioxy ring system to form hydrogen bonds. *β*-Caryophyllene, a non-polar hydrocarbon, is the weakest binder, interacting solely through dispersion forces and exhibiting a flexible, less stable docking pose. These findings indicate that successful SrtA inhibition requires not only favorable steric complementarity but also key interactions, such as hydrogen bonding, within the catalytic pocket.

Assessment of the properties of ADMET is a crucial step in early-stage drug discovery. This process enables the selection of compounds that exhibit optimal pharmacokinetic behavior and minimal safety concerns. Nine bioactive compounds derived from *P. betle* L. were evaluated using the pkCSM predictive platform.

All compounds, except for β-caryophyllene, fully complied with Lipinski's Rule of Five, indicating favorable oral bioavailability and drug-like properties. While β-caryophyllene exceeded the optimal lipophilicity threshold (logP > 5), it still exhibited high predicted intestinal absorption. All compounds consistently showed excellent intestinal absorption (>91%) and moderate-to-high Caco-2 permeability, supporting their potential for oral delivery. Furthermore, none were predicted to interact with P-glycoprotein (P-gp), thus alleviating concerns regarding efflux-related bioavailability issues.

Predicted BBB permeability varied among the compounds. β-Caryophyllene exhibited the highest BBB penetration potential, suggesting possible applications in CNS targeting; it also raised concerns about off-target effects. In contrast, acetyleugenol showed low BBB permeability, making it suitable for treating non-CNS infections while minimizing CNS exposure.

Metabolic interaction profiles revealed that six compounds—chavicol, chavibetol, eugenol, methyleugenol, estragole, and safrole—may inhibit the cytochrome P450 isoenzyme CYP1A2. Because CYP1A2 is responsible for metabolizing approximately 9% of clinically used drugs, including certain antidepressants and bronchodilators, this raises concerns regarding potential drug-drug interactions. Conversely, hydroxychavicol, acetyleugenol, and β-caryophyllene were not predicted to inhibit any major CYP isoforms, suggesting a reduced risk of metabolic interference and making them more suitable for further development, particularly in polypharmacy settings. Clearance predictions showed moderate variability among the compounds. β-Caryophyllene exhibited the highest clearance rate, indicating rapid systemic elimination, which may require more frequent dosing. Safrole demonstrated lower clearance, potentially leading to prolonged systemic exposure and increasing safety concerns. Integrating these findings with previous molecular docking results revealed that acetyleugenol was the most promising candidate, with the highest binding affinity to SrtA (S score = -5.98 kcal/mol) and excellent ADMET characteristics. Hydroxychavicol also showed a strong safety profile with no predicted toxicity, although its binding affinity was lower (S score = -4.84 kcal/mol), making it a good candidate for optimization. β-Caryophyllene, while lacking polar functional groups, maintains good absorption but has high clearance and BBB permeability, which may limit its systemic use. Methyleugenol, despite a strong binding affinity (S score = -5.39 kcal/mol), faces challenges owing to predicted mutagenicity and CYP1A2 inhibition. Safrole, while well absorbed, has significant safety liabilities owing to mutagenic and hepatotoxic potential. In conclusion, acetyleugenol and hydroxychavicol are the best candidates for further study, whereas other compounds require structural modifications to address safety concerns.

To further investigate the dynamic behavior and stability of the SrtA–ligand complexes identified through molecular docking, we conducted MD simulations using the CABS-flex 2.0 coarse-grained modeling platform. This approach assessed the impact of ligand binding on the conformational flexibility of SrtA by analyzing the RMSF profiles of all residues, with a special focus on the catalytic triad residues His120, Cys184, and Arg197. Low RMSF values indicate decreased atomic fluctuations and enhanced local stability, suggesting the restrained dynamics of key residues and potential inhibitory effects.

The RMSF profile of SrtA in complex with the natural substrate analog LPXTG showed typical flexibility in loop regions near residues Ala70, Ala105–115, Ala130, and Ala165–175, consistent with an active enzyme conformation. The catalytic triad residues exhibited low RMSF values (His120 = 0.447 Å, Cys184 = 0.231 Å, and Arg197 = 0.395 Å), indicating a stable active site environment.

Among *P. betle* L. compounds, acetyleugenol significantly stabilized Cys184 (RMSF = 0.261 Å) and moderately stabilized Arg197 (RMSF = 0.498 Å), resembling the LPXTG control complex. His120 was more flexible (RMSF = 0.788 Å); however, the observed decrease in flexibility and enhanced stability at Cys184 and Arg197 suggests that acetyleugenol may interact with the catalytic site in a manner consistent with the reference substrate pose. Chavicol demonstrated strong stabilization across the catalytic triad (His120 = 0.208 Å, Cys184 = 0.289 Å, and Arg197 = 0.402 Å), suggesting that despite a moderate docking score, it can restrict enzymatic dynamics. Safrole had the lowest RMSF for Cys184 (0.146 Å) and stabilized His120 (0.323 Å),

though its known mutagenic and hepatotoxic properties limit its potential use. Methyleugenol stabilized His120 (0.484 Å) and Arg197 (0.376 Å) but exhibited increased flexibility at Cys184 (0.675 Å), which may compromise the inhibitory efficacy. Eugenol, chavibetol, and β-caryophyllene showed moderate stabilization effects with RMSF values ranging from 0.3 to 0.6 Å, with β-caryophyllene notably stabilizing Arg197 (0.338 Å), indicating partial stabilization of the catalytic site. Conversely, estragole and hydroxychavicol increased the flexibility of critical residues His120 and Cys184, indicating weaker binding and docking affinities. This comprehensive in silico study integrates molecular docking, ADMET profiling, and MD simulations to identify several promising *Staphylococcus aureus* SrtA inhibitors from the bioactive compounds in *Piper betle* L. Among these, acetyleugenol emerged as the most compelling candidate, demonstrating strong docking affinity, favorable pharmacokinetic properties, and minimal safety concerns. MD simulations further supported its potential by showing significant stabilization of the crucial catalytic residue Cys184, which is essential for enzymatic function.

In addition, hydroxychavicol exhibited a favorable safety profile, making it suitable for further structural optimization. Notably, chavicol showed remarkable dynamic stabilization of catalytic residues, suggesting potential inhibitory efficacy despite a moderate docking affinity.

Antibacterial and antioxidant activity of P. betle

This study confirms the antibacterial activity of *P. betle* leaves on *S. mutans*. The extract inhibited *S. mutans* growth as shown by the growth inhibition zone, MIC and MBZ values. DNA leakage assay has been used to reveal how antibacterial drugs affect bacterial cell membrane.[15, 16] DNA and protein leakage is a direct indicator of the integrity of the bacterial cell membrane.[15] Previously, it was reported that dead cells released DNA, RNA, and protein fragments into the extracellular space, which was associated with membrane damage.[22] The results herein confirm the antibacterial activity of *P. betle* which is likely due to the disruption of *S. mutans* cell membrane.

Bioactive compounds in *P. betle* may contribute to the antibacterial activity. Hydroxychavicol causes oxidative stress in *E. coli* that precedes membrane damage, followed by DNA damage/repair.[23] Cell permeabilization was inhibited by Mg (II), and enhanced by the addition of EDTA. This finding suggests that hydroxychavicol damages the outer membrane of *E. coli*.[23]

In addition to the antibacterial activity, the antioxidant activity of *P. betle* leaves was investigated. Strong radical scavenging activities were obtained when tested based on DPPH and ABTS assays, with results comparable with those observed for Trolox. Eugenol which is one of the main compounds in *P. betle* had ABTS radical scavenging activity, with IC_{50} of 50 µg/mL [24] and less than 100 µM by DPPH assay.[25] A Strong scavenging effect on DPPH radicals was also reported by other researchers for eugenol and estragole, with EC_{50} (efficient concentration) ranging from 12.5 to 50 µM.[26] However, limited studies have been reported on the radical scavenging effect of chavicol. A derivative of chavicol had an IC_{50} of 312.50 µg/mL against DPPH radicals.[27]

Conclusion

The findings of this study highlight the therapeutic potential of bioactive constituents from *Piper betle* L., particularly acetyleugenol, as promising leads for novel antivirulence agents targeting SrtA in *S. aureus*. This antivirulence strategy offers a potential approach to mitigating conventional antibiotic resistance mechanisms. Although the computational predictions and biological models involve different bacterial species, the convergence of docking results with observed in vitro antibacterial effects provides a rational foundation for further validation of SrtA-specific inhibition in *S. aureus*. Nevertheless, the inherent limitations of the computational methods underscore the need for rigorous experimental verification. Furthermore, the strong antioxidant and antibacterial activities detected in *P. betle* leaf extracts suggest a synergistic effect of its bioactive compounds, contributing to bacterial growth inhibition and oxidative damage mitigation, supporting its traditional medicinal usage. Overall, these results position *P. betle* as a valuable natural resource for developing multi-target antivirulence agents with potential applications in combating resistant *S. aureus* infections.

Conflict of Interest

The authors declare no conflict of interest.

Authors' Declaration

The authors hereby declare that the work presented in this article is original and that any liability for claims relating to the content of this article will be borne by them.

Acknowledgements

This work was supported by Universitas Kristen Krida Wacana (UKRIDA) under grant No. 11/UKKW/LPPM-FKIK/LIT/10/2023.

References

1. Walsh TR, Gales AC, Laxminarayan R, Dodd PC. Antimicrobial Resistance: Addressing a Global Threat to Humanity. PLOS Med. 2023; 20(7): e1004264.
2. Tauran PM, Djaharuddin I, Bahrun U, Nurulita A, Katu S, Muchtar F, Pelupessy NM, Hamers RL, Day NPJ, Arif M, Limmathurotsakul D. Excess mortality attributable to antimicrobial-resistant bacterial bloodstream infection at a tertiary-care hospital in Indonesia. PLOS Glob Public Health. 2022; 2(7): e0000830.
3. Cheung GY, Bae JS, Otto M. Pathogenicity and virulence of *Staphylococcus aureus*. Virulence. 2021; 12(1): 547-569.
4. Turner NA, Sharma-Kuinkel BK, Maskarinec SA, Eichenberger EM, Shah PP, Carugati M, Holland TL, Fowler VG. Methicillin-resistant *Staphylococcus aureus*: An Overview of basic and clinical research. Nat Rev Microbiol. 2019; 17(4): 203-218.
5. Zong Y, Bice TW, Ton-That H, Schneewind O, Narayana SVL. Crystal structures of *Staphylococcus aureus* sortase A and its substrate complex J Biol Chem. 2004; 279(30): 31383-31389.
6. Thappeta KRV, Zhao LN, Nge CE, Crasta S, Leong CY, Ng V, Kanagasundaram Y, Fan H, Ng SB. In-Silico identified new natural Sortase A inhibitors disrupt *S. aureus* biofilm formation. Int J Mol Sci. 2020; 21(22): 8601.
7. Scharnow AM, Solinski AE, Wuest WM. Targeting *Streptococus mutans* biofilms: A Perspective on preventing dental caries. Medchemcomm. 2019; 10(7): 1057-1067.
8. Fernandes Forte CP, Oliveira FAF, Lopes CdB, Alves APNN, Mota MRL, de Barros Silva PG, Montenegro RC, Campos Ribeiro dos Santos ÂK, Lobo Filho JG, Sousa FB. *Streptococcus mutans* in atherosclerotic plaque: Molecular and immunohistochemical evaluations. Oral Dis. 2022; 28(6): 1705-1714.
9. Lin Y, Chen J, Zhou X, Li Y. Inhibition of *Streptococcus mutans* biofilm formation by strategies targeting the metabolism of exopolysaccharides. Crit Rev Microbiol. 2021; 47(5): 667-677.
10. Nayaka NMDMW, Sasadara MMV, Sanjaya DA, Yuda PESK, Dewi NLKAA, Cahyaningsih E, Hartati R. *Piper betle* (L): Recent review of antibacterial and antifungal properties, safety profiles, and commercial applications. Molecules. 2021; 26(8): 2321.
11. Chen CY-C. TCM Database@Taiwan: The World's Largest Traditional Chinese Medicine Database for Drug Screening In Silico. PLOS ONE. 2011; 6(1): e15939.
12. Erlina L, Paramita RI, Kusuma WA, Fadilah F, Tedjo A, Pratomo IP, Ramadhanti NS, Nasution AK, Surado FK, Fitriawan A, Istiadi KA, Yanuar A. Virtual screening of Indonesian herbal compounds as COVID-19 supportive therapy: Machine learning and pharmacophore modeling approaches. BMC Complement Med Ther. 2022; 22(1): 207.
13. Molecular Operating Environment. Chemical computing group ULC: Molecular Operating Environment Montreal, Quebec, Canada; 2022.
14. Simamora A, Santoso AW, Rahayu I, Timotius KH. Enzyme inhibitory, antioxidant, and antibacterial activities of ethanol fruit extract of *Muntingia calabura* Linn. J Herbmed Pharmacol. 2020; 9(4): 346-354.

15. Topçu S, Şeker MG. In Vitro antimicrobial effects and inactivation mechanisms of 5,8-dihydroxy-1,4-napthoquinone. Antibiotics. 2022; 11(11): 1537.
16. Shalini V, Shanmugam R, Manigandan P. Cytoplasmic leakage and protein leakage analysis of *Ocimum gratissimum* stem extract-mediated silver nanoparticles against wound pathogens. J Pharm Bioallied Sci. 2024; 16(Suppl 2): S1354-S1359.
17. Simamora A, Timotius KH, Setiawan H, Ningrum RA, Mun'im A. Characteristics of xanthorrhizol rich extract from *Curcuma xanthorrhiza* in the choline chloride-based natural deep eutectic solvents: DNA protective activity and toxicity profiles. Int J Agric Biol. 2024; 32(3): 249-260.
18. Hikmawanti NPE, Saputri FC, Yanuar A, Jantan I, Ningrum RA, Juanssilfero AB, Mun'im A. Choline chloride-urea-based natural deep eutectic solvent for highly efficient extraction of polyphenolic antioxidants from *Pluchea indica* (L.) Less leaves. Arabian J Chem. 2024; 17(2): 105537.
19. Tran VT, Nguyen TB, Nguyen HC, Do NHN, Le PK. Recent applications of natural bioactive compounds from *Piper betle* (L.) leaves in food preservation. Food Control. 2023; 154: 110026.
20. Ratchasong K, Saengsawang P, Yusakul G, Makkliang F, Lakhanapuram HK, Wintachai P, Thomrongsuwannakij T, Nwabor OF, Punyapornwithaya V, Romyasamit C, Mitsuwan W. Bactericidal activities of nanoemulsion containing *Piper betle* L. leaf and hydroxychavicol against avian pathogenic *Escherichia coli* and modelling simulation of hydroxychavicol against bacterial cell division proteins. Antibiotics. 2025; 14(8): 788.
21. Risdian C, Widowati W, Mozef T, Wargasetia TL, Khiong K. Free radical scavenging activity of ethanolic leaves extract and its different solvent fractions of *Piper betle* L. in vitro. Indones J Cancer Chemoprevention. 2011; 2(1): 141-145.
22. Sato A, Shimotsuma A, Miyoshi T, Takahashi Y, Funayama N, Ogino Y, Hiramoto A, Wataya Y, Kim H-S. Extracellular leakage protein patterns in two types of cancer cell death: necrosis and apoptosis. ACS Omega. 2023; 8(28): 25059-25065.
23. Singh D, Majumdar AG, Gamre S, Subramanian M. Membrane damage precedes DNA damage in hydroxychavicol treated *E. coli* cells and facilitates cooperativity with hydrophobic antibiotics. Biochimie. 2021; 180: 158-168.
24. Lima JAC, de Farias Silva J, de Moraes MM, de Araujo CA, da Câmara CAG, Freitas JCR. In vitro evaluation of the antioxidant potential of derivatives eugenol via ABTS radical capture assay. Acta Brasiliensis. 2023; 7(3): 80-84.
25. d' Avila Farias M, Oliveira PS, Dutra FSP, Fernandes TJ, de Pereira CMP, de Oliveira SQ, Stefanello FM, Lencina CL, Barschak AG. Eugenol derivatives as potential anti-oxidants: is phenolic hydroxyl necessary to obtain an effect? J Pharm Pharmacol. 2014; 66(5): 733-746.
26. Tominaga H, Kobayashi Y, Goto T, Kasemura K, Nomura M. DPPH radical-scavenging effect of several phenylpropanoid compounds and their glycoside derivatives. Yakugaku zasshi. 2005; 125(4): 371-375.
27. Santos BCS, Pires AS, Yamamoto CH, Couri MRC, Taranto AG, Alves MS, Araújo ALdSdM, de Sousa OV. Methyl chavicol and its synthetic analogue as possible antioxidant and antilipase agents based on the in vitro and in silico assays. Oxidative Med Cell Longev. 2018; 2018(1): 2189348.